Identification of the Fortnightly Wave Observed Along the Northern Coast of the Gulf of Guinea

ALLAN J. CLARKE

Department of Oceanography, The Florida State University, Tallahassee, FL 32306

DAVID S. BATTISTI

Department of Atmospheric Sciences, University of Washington, Seattle, WA 98195

(Manuscript received 29 November 1982, in final form 15 July 1983)

ABSTRACT

Numerical calculations of coastally trapped wave modes along the northern coast of the Gulf of Guinea using representative bottom topography and continuous stratification on a β-plane were carried out to identify the observed fortnightly propagating coastal wave. Results showed that the propagation speed of the observed wave (approximately 53 cm s^{-1} for sea level and 54 cm s^{-1} for sea surface temperature) is close to that of the second mode (64 cm s^{-1}) and no other. Off the shelf this mode has a baroclinic structure, having considerable amplitude at 2 km depth. Ray theory calculations indicate that if, as is likely, the observed wave were generated on the shelf, a vertically standing modal structure with large amplitude at 2 km depth is not possible. Therefore, no coastally trapped vertically standing wave modes are consistent with the observed wave. Consequently, it is most likely that the wave is a vertically propagating coastally trapped wave as has been observed recently in other contexts. There is some evidence suggesting that the wave is generated by the nonlinear interaction of the M_2 and S_2 tides due to bottom friction on the wide shelf in the northeastern corner of the Gulf.

1. Introduction

Long time series of coastal sea level observations in the Gulf of Guinea indicate that a wave at 14.7-day period propagates along the coastline between Lome and Monrovia with a mean phase speed of 53 cm s^{-1} [see Figs. 1, 2, and Picaut and Verstraete (1979)]. This wave is strongly baroclinic (Houghton and Beer, 1976; Picaut and Verstraete, 1979), has the same frequency as the luni-solar (MS_f) tide, and has a sea level amplitude more than seven times that of the equilibrium tide. How and where the wave is generated are still open questions, but Picaut and Verstraete (1979) suggest that the wave is generated by some nonlinear interaction of the M_2 and S_2 tides since

$$\omega(MS_f) = \omega(S_2) - \omega(M_2)$$
$$= (2\pi/14.7653)\ \text{day}^{-1}. \qquad (1.1)$$

In (1.1), $\omega(MS_f)$, $\omega(S_2)$ and $\omega(M_2)$ refer, respectively, to the frequencies of the MS_f, S_2 and M_2 tides.

The wave is one of the very few harmonic low frequency waves ever observed in the ocean and there have been several attempts to understand it theoretically. Suggestions for the type of wave seen propagating include a topographic shelf wave (Philander, 1977), an equatorial topographic wave (Mysak, 1978a, 1978b), an internal Kelvin wave (Houghton and Beer, 1976), and a coastally trapped topographic Rossby wave (Houghton, 1979).

There seem to be difficulties with all of the above suggestions. The barotropic waves ignore stratification and cannot explain the baroclinic effects of order zero of propagating sea surface temperature and fluctuating subsurface isotherms (Houghton and Beer, 1976; Picaut and Verstraete, 1979). On the other hand, Picaut and Verstraete (1979) have pointed out that when the stratification on the shelf changes during the upwelling season, the phase speed of the wave does not change. Therefore, Houghton (1979) concluded that the wave could not be an internal Kelvin wave because the phase speed of such a wave depends on the stratification. In fact, any wave that is significantly baroclinic should have a phase speed dependent on stratification and so, one might think, would show a speed change during the upwelling season. Hence, the observations seem to simultaneously demand and reject a wave with baroclinic properties, and this leaves one puzzled as to the wave type.

In this paper we attempt to identify the observed wave. None of the above suggested wave types was based on results of a model that included realistic topography, continuous stratification, and the β-effect. In the next section, theory and calculations for such a model are described. Then a comparison of theoretical results with observations follows in Section 3.

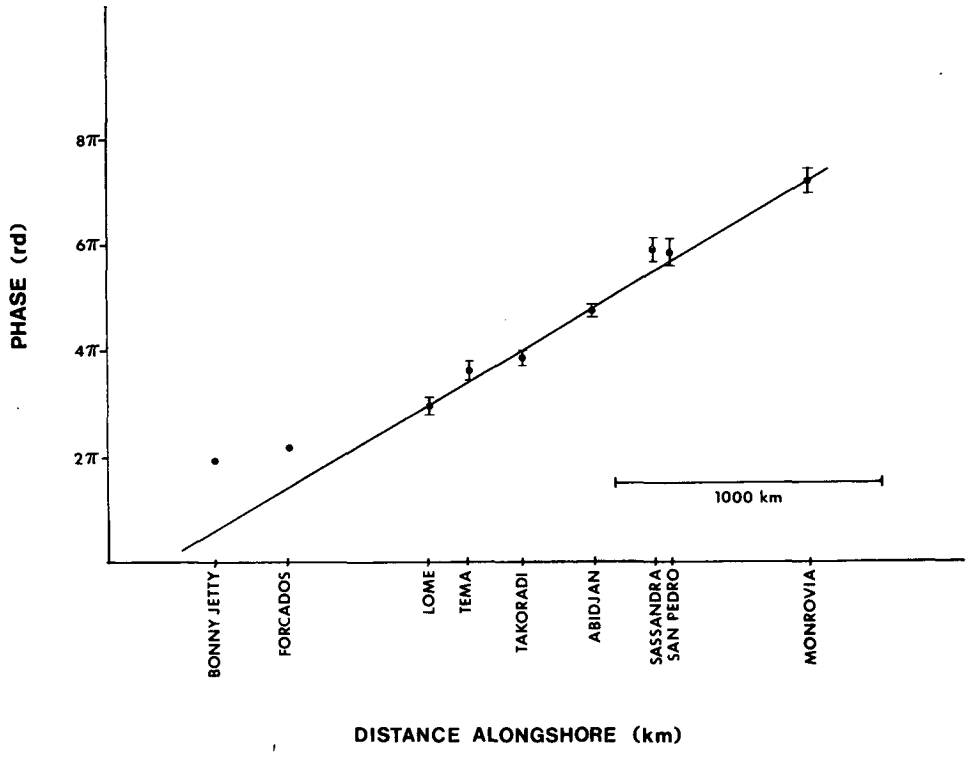

FIG. 1. Phase variation of the MS_f tide along the coast in the Gulf of Guinea. An explanation of the error estimates is given in Picaut and Verstraete (1979). Two stations, Bonny Jetty and Forcados, have been added to the graph. Results for these stations were obtained from the International Hydrographic Bureau. No error estimates were available. Bonny Jetty and Forcados may be in the region of generation of the wave and so the phase of the MS_f tide at these locations does not fall on the straight line corresponding to free wave propagation. The straight line fit corresponds to a phase speed of 53 cm s^{-1}. (Adapted from Picaut and Verstraete, 1979).

Section 4 contains a discussion on the generation of the wave. A summary and concluding remarks are found in Section 5.

2. Theory

The observed 14.7-day wave propagates in the direction and at about the phase speed that one might expect the lowest order coastally trapped free waves to propagate. This suggests that one should look for the freely propagating wave solutions.

Clarke (1977), Huthnance (1978), Wang and Mooers (1976), Brink (1982a), Ou (1980), Ou and Beardsley (1980) and Chapman and Hendershott (1982) have all discussed coastally trapped waves on an f-plane for continuous stratification and various shelf topographies. In the calculations to follow the β-plane effect has also been included, as at the low latitudes of interest here (5°N) this term will significantly change the phase speed of the calculated trapped waves. For the numerical calculations we used a numerical model developed by Brink (1982b). The model computes, for an east-west coastline, the free coastally trapped wave dispersion curves and modal structures for general stratification and seaward shelf topography on a β-plane using a resonance iteration technique on a vertically stretched grid (25 points offshore and 17 points in the vertical). The equations solved by the model are given in Appendix B.

The free-wave solutions were calculated using a bottom topography profile off Tema, Ghana (see Figs. 2, 3). This shelf topography is representative of the Gulf of Guinea shelf topography from Lagos to Monrovia (excluding the wide shelf off Takoradi). The shelf is narrow, with depth increasing rapidly once off the shelf break (23 km from shore). The density data used to calculate the Brunt–Väisälä frequency N (see Fig. 3c) were obtained from Houghton (1976), Longhurst (1962), Duing *et al.* (1980) and Fuglister (1960). Houghton documents the density structure from the surface to a depth of 260 m at the shelf break off Tema and also finds that, except in the upwelling season, the stratification is virtually horizontal from the coast to well past the shelf break. The data from Longhurst, Fuglister and Duing *et al.* were used to estimate the structure below 300 m to the ocean floor. The Brunt–Väisälä frequency profile off Tema is fairly representative of that along the northern coast of the Gulf of

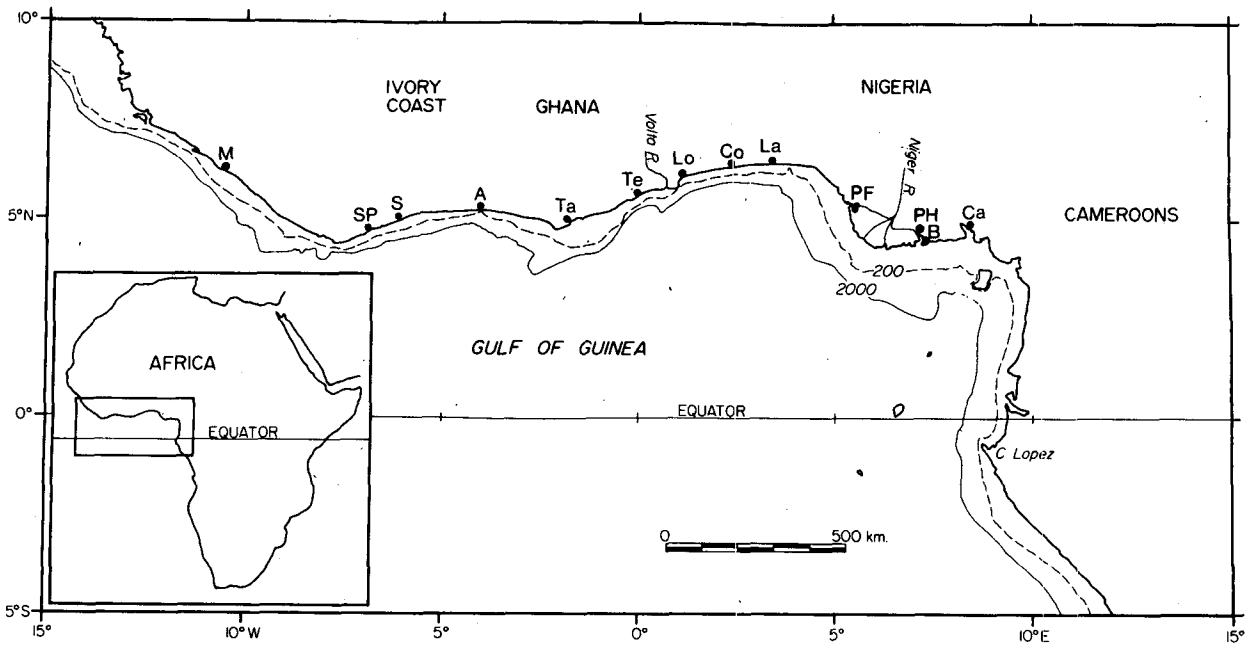

FIG. 2. The Gulf of Guinea shelf bathymetry (depth contours in meters). Also plotted are towns where relevant sea level measurements are available. M = Monrovia, SP = San Pedro, S = Sassandra, A = Abidjan, Ta = Takoradi, Te = Tema, Lo = Lome, Co = Cotonou, La = Lagos, PF = Port of Forcados, PH = Port Harcourt, B = Bonny Jetty, Ca = Calabar. (Adapted from Picaut and Verstraete, 1979).

Guinea except in the upper 150 m. However, results (see Section 3) show that changes in the stratification in the upper 150 m do not affect phase speeds of the lower modes, so ignorance of the precise profile in the upper 150 m is not a serious problem.

3. Discussion of the theoretical results and observations

a. Explanation of the observed wave as a mode 2 coastally trapped wave

The calculated dispersion curves for the representative values of stratification and topography off Tema, Ghana, are shown in Fig. 4. One can see that at the MS_f frequency at least two modes can exist. The extremely small value of f at this latitude together with the large wave number at $\omega = \omega(MS_f)$ for mode 3 and the higher modes make it difficult to numerically ascertain the characteristics of the third or higher modes. The results of Chapman (1983) show that the frictionless f-plane version of these modes exist at the MS_f frequency. However, even if these modes exist at the MS_f frequency in the more realistic frictional β-plane case, they are not of direct interest here since their phase speed is very different from that observed. In fact, since the observed phase speeds are, for sea level, 0.53 m s^{-1} (Picaut and Verstraete, 1979) and for sea surface temperature, 0.54 and 0.64 $\pm$ 0.12 m s^{-1} (Picaut and Verstraete, 1979; Houghton and Beer, 1976), only mode 2 (phase speed 0.64 m s^{-1}) has a speed near the observed speed (mode 1's is 1.31 m s^{-1}). It is worth pointing out here the significant influence of the earth's curvature (β-effect) on the theoretical mode 2 phase speed; the speed is reduced -20% from that calculated for an f-plane.

The numerical model's predictions for the longshore current for mode 2 at the MS_f frequency are documented in Fig. 5. In some ways the velocity structure is like that of a second mode deep sea internal Kelvin wave. Specifically, the energy is trapped to the coast with a horizontal decay scale approximately that of the mode 2 Kelvin wave, and the zeros in longshore velocity are nearly horizontal. But it should be stressed that the mode 2 coastal trapped wave has zeros at different depths to the mode 2 Kelvin wave and also has other properties significantly different from the mode 2 Kelvin wave. For example, the phase speed is quite different (see Fig. 4) due to the influence on mode 2 of bottom topography and the curvature of the earth (β-effect). The significant influence of bottom topography is consistent with the baroclinic radius of deformation for the second mode Kelvin wave (a_2) being comparable to the cross shelf and continental slope topographic scale (L); a Kelvin wave like mode would require $a/L \gg 1$, the nearly vertical wall case.

How baroclinic is the mode 2 coastally trapped wave? The ratio of the kinetic energy of a coastally trapped wave to its potential energy is a measure of baroclinicity. This ratio is 1 for a baroclinic coastal Kelvin wave and ∞ for a nondivergent barotropic shelf wave (see Brink, 1982b) so the value 1.7 for mode 2 indicates that it is strongly baroclinic. This is consistent

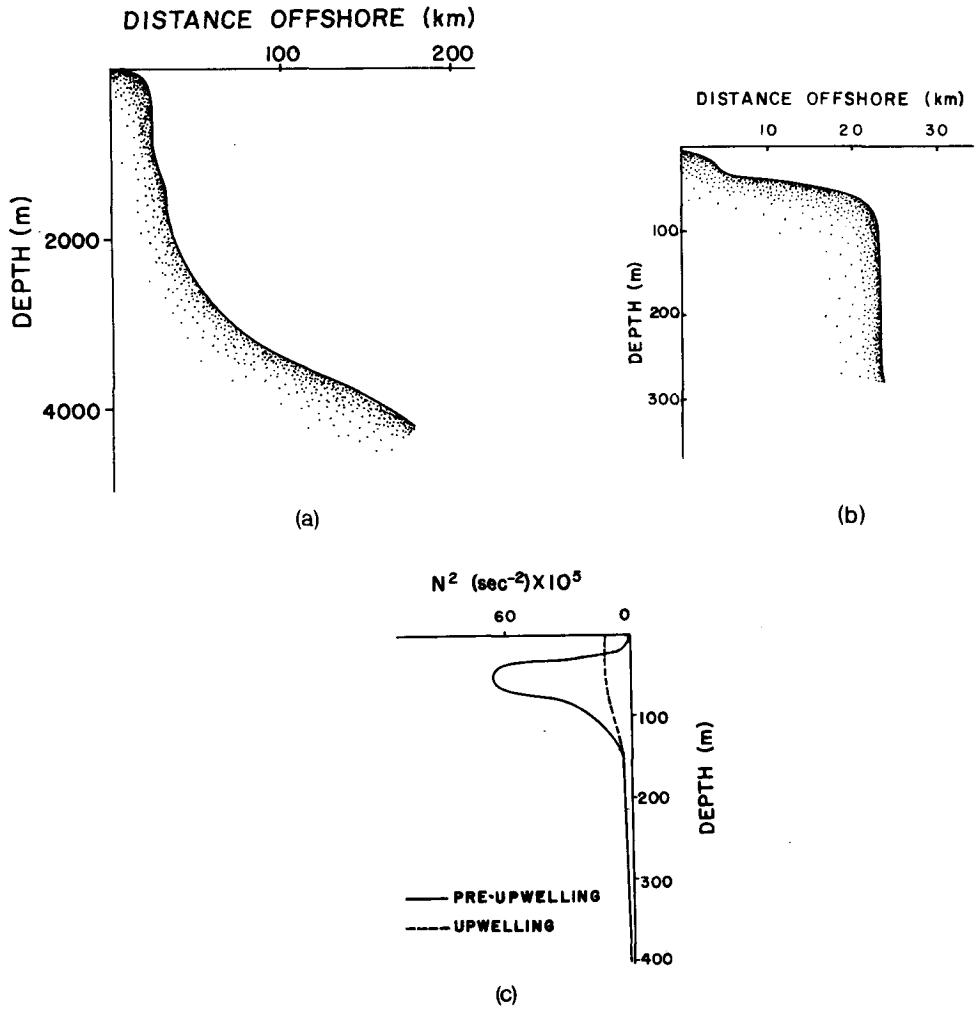

FIG. 3. (a) Bathymetry profile off Tema, Ghana; (b) nearshore detail of the bathymetry; and (c) profile of N^2 as a function of depth. Below 400 m, $N^2(z) = N^2(400\text{ m})\exp[(z + 400\text{ m})\alpha]$ with $\alpha^{-1} = 1070$ m, $N^2(400\text{ m}) = 1.2 \times 10^{-5}\text{ s}^{-2}$.

with the observed propagation of sea surface temperature fluctuations (Houghton and Beer, 1976) and thermocline fluctuations (Picaut and Verstraete, 1979). But if the wave is, in fact, baroclinic, why does the observed phase speed of the wave not change significantly during the upwelling season when the stratification changes? To examine this question, calculations were performed for stratification typical of the non-upwelling and upwelling season (see Fig. 3). The phase speeds obtained were 0.64 m s^{-1} (non-upwelling season) and 0.61 m s^{-1} (upwelling season). These phase speeds are close enough that, within the limits of observational error, no phase speed change should have been observed. The reason for the negligible change in phase speed is that the wave owes its phase speed mostly to the stratification in deep water beneath about 150 m and this is virtually unchanged during the upwelling season. Note that since the phase speed depends on the stratification beneath 150 m, it is inappropriate to model stratification, even in the non-upwelling season, as two layers with a density jump at $\approx$40 m.

b. *Difficulties with the mode 2 coastally trapped wave interpretation*

Despite the good agreement between theory and observation for the mode 2 coastally trapped wave, there are serious difficulties with such an interpretation. These are discussed below.

1) MODE 2 HAS NO VERTICAL PHASE PROPAGATION

It seems probable that the observed MS_f tide is generated in shallow water (see Section 4). But if it is, then we need to explain how the energy predicted to occur at greater than 2 km depth (see Fig. 5) gets there. Theory suggests (Romea and Allen, 1983) that motions generated near the surface in stratified water adjacent to a coastal wall propagate vertically. The mode 2

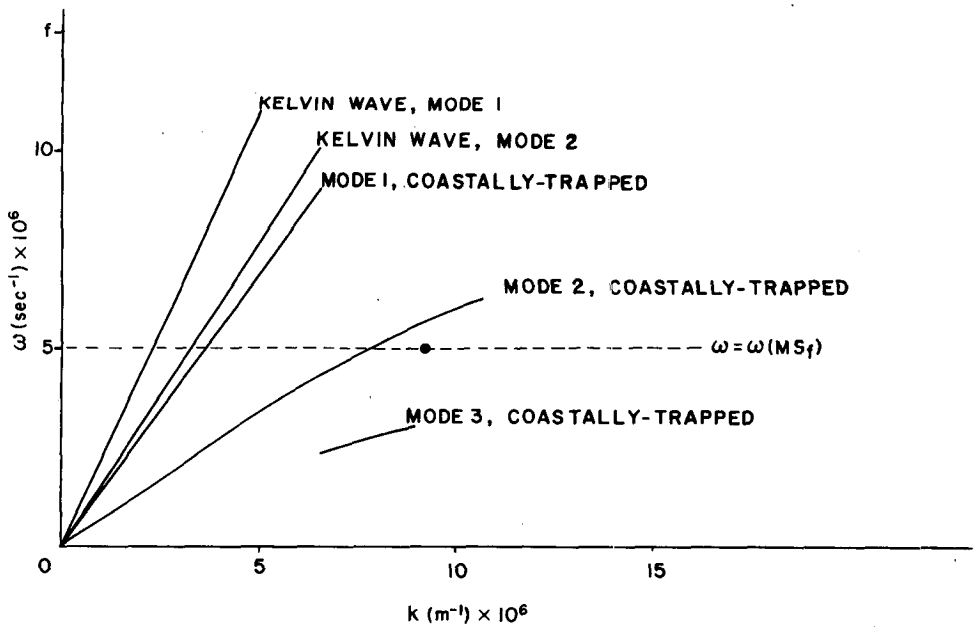

FIG. 4. Dispersion diagram for coastal-trapped modes 1 and 2 off Tema. Also plotted are the deep sea internal coastal Kelvin wave solutions (modes 1 and 2) for the same $N^2(z)$ profile. The heavy dot signifies (ω, k) corresponding to the MS_f tide with phase speed 0.53 m s^{-1}.

coastally trapped wave has no phase propagation in the vertical—it is a vertically standing mode. For a vertically standing mode interpretation to be valid the angle of vertical propagation to the horizontal must be steep enough so that the horizontal distance d over which the energy propagates down, reflects from the bottom and reaches the surface again is very much less than a horizontal wavelength. Ray theory indicates that the angle of propagation to the horizontal for a wave of frequency ω is $\omega/N(z)$ and this enables us to estimate d. Calculations for 2 km depth using observed $N(z)$ and $\omega(MS_f)$ indicate that d is in fact greater than a wavelength. Thus the wave is likely to be in the form of a vertically propagating wave, at least over the continental slope. The mode 2 vertically standing wave interpretation therefore appears to be invalid.

Observational support for vertically propagating coastally trapped waves near the equator is available for other regions. Vertically propagating coastally trapped waves have been observed with periodicity of approximately a few weeks and longer off the coast of Peru (see Romea and Allen, 1983) and at a lower frequency for the northern coast of the Gulf of Guinea (Picaut, 1983).

2) A MODE 2 VERTICALLY STANDING WAVE DOES NOT APPEAR TO EXPLAIN SEA LEVEL AMPLITUDE CHANGES ALONG THE COAST

Examination of Fig. 6 indicates that the sea level amplitude varies considerably and nonsystematically with distance along the coast. The mode 2 coastally trapped freely propagating wave can, in theory, have its coastal sea level amplitude changed because of longshore variations in stratification and topography. Energy Flux Theory derived in Appendix A can be used to find coastal sea level amplitude changes when topography and stratification vary alongshore, and we found that changes were negligible except in a small region near Takoradi. There changes in continental slope topography resulted in amplification by a factor 1.6. Note that changes longshore in stratification were not known, but we suspect that such changes are confined to the upper few hundred meters and these changes do not significantly affect coastal sea level amplitudes. Thus it appears that the mode 2 wave cannot explain sea level amplitude variations along the coast (see Fig. 6).

3) OBSERVED AND MODE 2 LONGSHORE CURRENT STRUCTURES DISAGREE AT THE SHELF BREAK

Houghton (1979) has reported current meter measurements at the shelf edge off Tema for the fortnightly tide. The observations suggest that the longshore current near the shelf break has considerable vertical structure, whereas the mode 2 longshore current is fairly uniform vertically at the shelf break. This discrepancy, while possibly due to errors in the mode 2 calculations because of the difficulty in resolving the shelf break numerically, nevertheless casts further doubt on the mode 2 explanation of the observed wave.

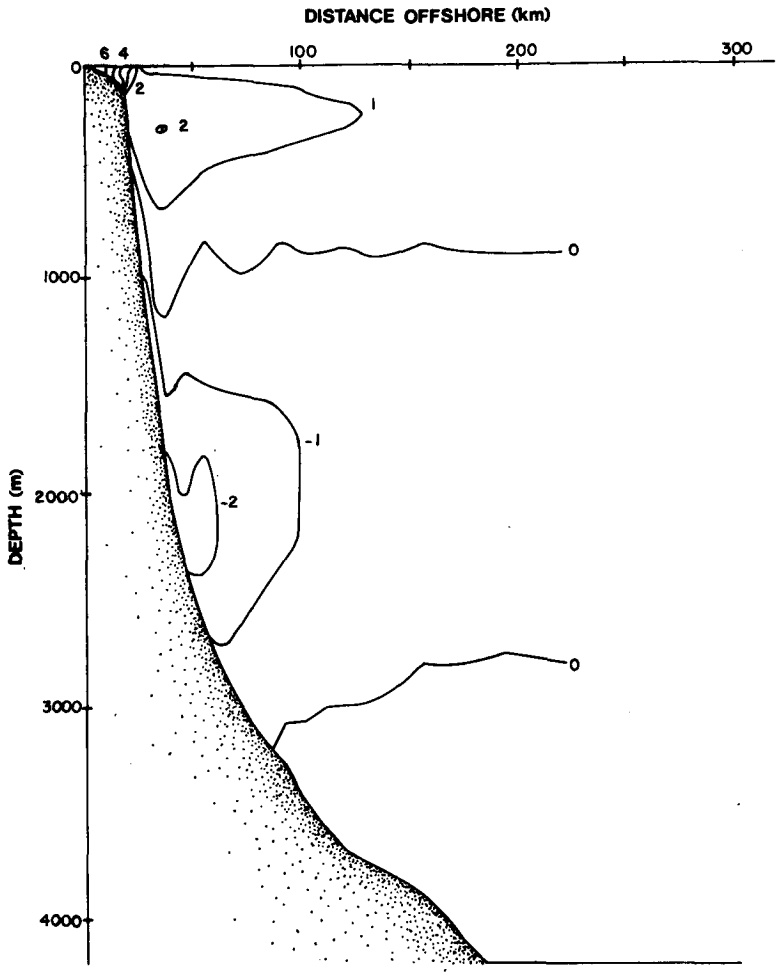

FIG. 5. Vertical cross section of the longshore velocity v (cm s^{-1}) for the mode 2 coastal-trapped wave at the MS_f frequency off Tema, Ghana. Velocity amplitudes are based on the assumption that the observed MS_f sea level amplitude at the coast is entirely due to the mode 2 coastal-trapped wave.

c. *The vertically propagating coastally trapped wave interpretation*

Section 3b suggests that the observed wave is not a mode 2 coastally trapped wave. It appears, therefore, that no *single* standing vertical coastally trapped wave fits the observations. Consequently it seems that the observed propagation must be due to a sum of standing coastally trapped waves. From Section 3b.1 we expect that this sum should form a vertically propagating coastally trapped wave. Such an interpretation is consistent with strong variations in amplitude along the coast (see Section 3b.2) because a vertically propagating wave, reflecting from bottom topography and the ocean's surface sometimes has its energy concentrated near the surface and sometimes not.

It is less obvious that other properties of the vertically propagating wave are consistent with observation. For example, since the exact combination of modes is not known (because details of the generation mechanism for the wave is not known) it is not possible to predict the wave's phase speed. It is also not possible to verify that the vertically propagating wave's phase speed is virtually independent of changes in stratification in the upper 150 m as the mode 2 phase speed is, although this is likely, because it is likely that all coastally trapped waves making up the sum have phase speeds virtually independent of stratification in the upper 150 m. This conclusion is based on the fact that all the internal Kelvin wave modes have this property.

4. Generation of the wave

Since the group velocity of the wave is westward (see Fig. 4), the wave must be generated in the eastern part of the Gulf of Guinea or even earlier along the wave guide, viz., along the equator. It seems unlikely that the signal could have come from the equatorial

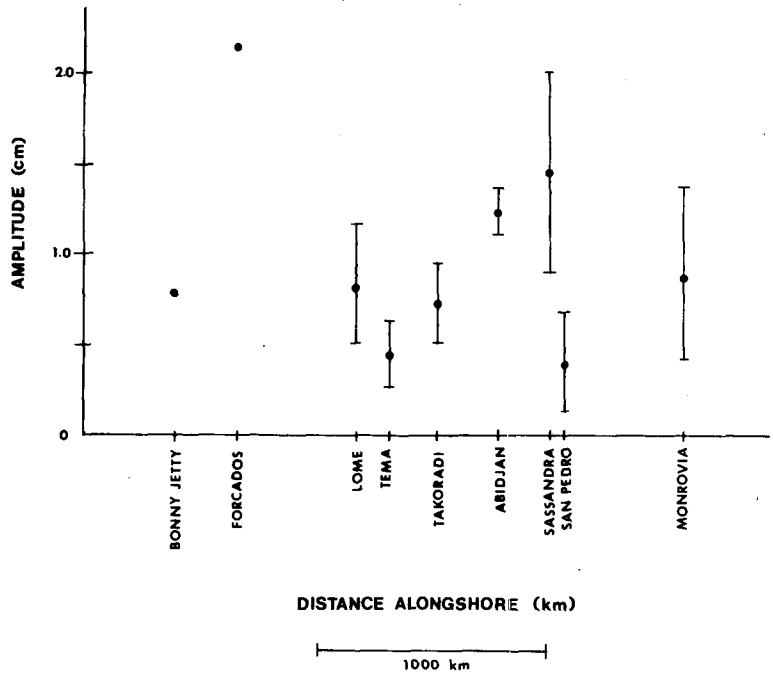

FIG. 6. MS_f sea level amplitude versus distance along the coast. The data were taken from Table 5 of Picaut and Verstraete (1979) and the International Hydrographic Bureau (IHB). The IHB data did not have error estimates.

wave guide, since there the water is too deep for M_2 and S_2 tidal currents to be large enough to nonlinearly generate an MS_f signal of the magnitude observed. On the other hand, the large phase shifts and amplitude changes of Bonny Jetty and Forcados compared to the relatively smooth linear phase changes west of these stations suggest that the wave may be being generated in the wide shelf region adjacent to the Niger Delta (see Figs. 1 and 2). While this may be the case, it should be pointed out that we have no information as to the errors in the phases and amplitudes at these stations. Furthermore, the Bonny Jetty and Forcados stations are up inlets 9 km and 14 km from the open sea, respectively, and it is probable that these stations are influenced by the MS_f tide being generated in the inlet as well as the MS_f tide on the open shelf. Evidence for the influence of an inlet tide on the Bonny Jetty station data is, for example, given by the 5.4 cm MS_f tide at Port Harcourt, ~36 km farther up the inlet from Bonny Jetty.

In spite of the uncertainty in the usefulness of the Bonny Jetty and Forcados data, we still suspect that the wave is being generated on the wide shelf adjacent to the Niger River Delta. Our reasoning is as follows. The shelf tidal theory of Clarke and Battisti (1981) and Battisti and Clarke (1982a, 1982b) indicates that barotropic coastal tidal M_2 and S_2 sea levels and currents should be significantly larger in the wide shelf region adjacent to the Niger Delta than elsewhere along the coast. The major reason for this is that there is a tendency for barotropic semidiurnal tides to be amplified on wide shelves with $\omega > f$. Due to the lack of coastal sea level data it is impossible to say exactly how much greater M_2 and S_2 tidal currents are in the proposed generation region, but the M_2 and S_2 barotropic currents should be a factor of at least 5 larger than their counterparts on the narrow part of shelf between Lome and Monrovia where the wave is seen to propagate. Since the forcing mechanism is nonlinear in the M_2 and S_2 currents, the forcing in the generation region is an order of magnitude larger than in the region where the shelf wave propagates freely. This is what one would expect if the hypothesis were true.

As stated above, the forcing mechanism is nonlinear in the M_2 and S_2 currents. The nonlinearity is either associated with the nonlinear momentum terms uu_x, vu_y, uv_x, vv_y, or the x component of the bottom stress, $\rho_0 C_D|\mathbf{u}|u$ (C_D = drag coefficient, ρ_0 = mean water density). Order of magnitude estimates of these terms suggest that it is the bottom friction term calculated in the shallow water near the coast that is most likely the dominant term in driving the MS_f tide.

5. Summary and concluding remarks

The main aim of this paper was to identify the fortnightly propagating coastal wave observed along the northern coastline of the Gulf of Guinea. We found, for a β-plane model incorporating realistic bottom topography and stratification, that the only mode with

speed close to that observed was the mode 2 coastally trapped wave. However, there were fundamental difficulties with a mode 2 coastally trapped wave interpretation, and it is more likely that the observed wave is a vertically propagating coastally trapped wave. Such an interpretation is consistent with observation, although confirmation awaits further measurement, and in particular measurement of vertical propagation. There is some evidence that the wave is generated on the wide shelf in the vicinity of the Niger Delta (see Fig. 2). The MS_f tide is probably generated nonlinearly by bottom friction effects through the interaction of the larger M_2 and S_2 tidal currents in this region.

Acknowledgments. This research was supported by NSF Grant OCE-8118051. We would also like to acknowledge the helpful discussions we had with Dr. Ken Brink and Dr. David Chapman while we were Guest Investigators at the Woods Hole Oceanographic Institution, summer 1982. Dr. Brink also generously provided us with the numerical model used for the calculations.

APPENDIX A

Estimating the Effect of Slowly Varying Longshore Topography and Coastline on Freely Propagating Coastally Trapped Wave Motions

As pointed out in Section 3, the strong variations in coastal sea level amplitude seen in Fig. 6 might be due to longshore variations in topography and coastline. To test this hypothesis, theory is developed below for calculating such sea level changes when coastline and longshore topography vary 'slowly' in the sense that longshore variations occur on a scale much larger than variations perpendicular to the coast. In practice this means that longshore scales of topography and coastline are much greater than the shelf width and baroclinic radius of deformation, the possible boundary layer trapping scales.

Beginning with the linearized Bousinesq equations of motion for a stratified ocean [e.g., see Gill and Clarke (1974), Eqs. (2.2)–(2.6)] with wind stress set equal to zero, one can derive the energy equation

$$\frac{\partial}{\partial t}\left[\frac{1}{2}\left(u^2+v^2+\frac{g^2\sigma^2}{\rho_0{}^2N^2}\right)\right]+\frac{1}{\rho_0}\nabla\cdot(p\mathbf{u})=0. \quad \text{(A1)}$$

In (A1) $t, u, v, g, \sigma, \rho_0, N, \nabla, p$, and $\mathbf{u}$ refer, respectively, to the time, the velocity component normal to the coast, the velocity component tangential to the coast, the acceleration due to gravity, the perturbation density, the mean (constant) density of the water, the buoyancy frequency, the three-dimensional gradient operator, the perturbation pressure and the three-dimensional velocity vector.

Consider normal and tangential coordinates (n, s) where n denotes distance from the coast and s distance along the coast. Let z be the vertically upward coordinate and let V be the volume bounded by the coast $n = 0$, the free surface $z = 0$, the ocean floor $z = -H(n, s)$ and planes $s = s_1$ and $s = s_2$ normal to the coastline. The seaward boundary of the volume V is effectively $n = \infty$ because of the assumption that longshore scales of variation in topography and coastline are much greater than the coastal boundary layer trapping scale.

Integrating over the volume V, one has, for time-averaged flows (the overbar denotes time average):

$$\int_V \nabla\cdot(\overline{p\mathbf{u}})dV=0. \quad \text{(A2)}$$

If the divergence theorem is applied to (A2) and then use is made of the boundary conditions of no normal flow through the surface, bottom and coast as well as $p = 0$ at $n = \infty$, one arrives at

$$\int_{s=s_1}\overline{pv}dS=\int_{s=s_2}\overline{pv}dS. \quad \text{(A3)}$$

Since $s = s_1$ and $s = s_2$ are arbitrary planes normal to the coast, (A3) is simply a statement that in the absence of dissipation or forcing, the energy flux is conserved through a plane normal to the coast.

Since longshore variations in topography and coastline are much greater than the shelf width and the baroclinic radius of deformation, for low-frequency motion

$$\frac{\partial}{\partial t}\frac{\partial}{\partial s}\left(f\frac{\partial}{\partial n}\right)^{-1}\ll 1;$$

consequently we can write

$$v=\frac{\partial p}{\partial n}f^{-1}. \quad \text{(A4)}$$

Thus we see that the energy flux can be written

$$\left[\int_{n=0}^{\infty}\int_{z=-H(n,s)}^{z=0}\overline{\frac{1}{f}\frac{\partial}{\partial n}\left(\frac{1}{2}p^2\right)}dzdn\right]_{s=\text{constant}}.$$

Alternatively, using

$$\frac{\partial}{\partial n}\left[\int_{-H(n,s)}^{0}\left(\frac{1}{2}p^2\right)dz\right]=\int_{-H(n,s)}^{0}\frac{\partial}{\partial n}\left(\frac{1}{2}p^2\right)dz+\frac{\partial H}{\partial n}\frac{1}{2}p^2\Big|_{z=-H}$$

and the boundary conditions $H|_{n=0}=0$ and $p|_{n=\infty}=0$, one concludes that

$$I=\left[\int_{n=0}^{n=\infty}\overline{p^2}\frac{\partial H}{\partial n}dn\right]_{s=\text{constant}} \quad \text{(A5)}$$

must be constant for any cross section s = constant. Further, if $H(n, s)$ is monotonic in n then p is a single-valued function of H and the integral in (A5) can be simplified to

$$\left[\int_{H=0}^{H_\infty} \overline{p^2(-H)}dH\right]_{s=\text{constant}}. \quad \text{(A6)}$$

As indicated in the text, Eq. (A5) and (A6) can be used to find out how pressure and, hence, sea level vary along the coast when the stratification and topography change smoothly alongshore.

APPENDIX B

The Coastally Trapped Wave Model Equations

The equations solved by the model (discussed in Section 2) result from the linearized Boussinesq equations of motion for a stratified ocean [e.g., see Gill and Clarke (1974), Eqs. (2.2)–(2.6)] with the wind stress set equal to zero. Elimination of all variables in favor of the pressure, written

$$p(x, y, z, t) = F(y, z)\exp(ikx + i\omega t), \quad \text{(B1)}$$

yields the following field equation for F:

$$(f_0^2 - \omega^2)\left(\frac{F_z}{N^2}\right)_z + F_{yy} - \frac{2f_0\beta}{(f_0^2 - \omega^2)}F_y + \left[\left(\frac{2f_0^2\beta k}{\omega(f_0^2 - \omega^2)}\right) - k^2 - \frac{\beta k}{\omega}\right]F = 0. \quad \text{(B2)}$$

In (B2), the Coriolis parameter f, is

$$f = f_0 + \beta y. \quad \text{(B3)}$$

The field equation is subject to no normal flow through the surface ($z = 0$), bottom $z = -h(y)$ and coast ($y = 0$) as well as a trapping condition that the pressure approaches zero at large distances from the coast. In terms of F, these conditions can be written

$$N^2 g^{-1}F + F_z = 0, \quad \text{(B4)}$$

$$(f_0^2 - \omega^2)F_z + N^2 h_y\left(F_y - \frac{f_0 k}{\omega}F\right) = 0, \quad \text{at} \quad z = -h(y), \quad \text{(B5)}$$

$$F_y - \frac{kf_0}{\omega}F = 0, \quad \text{at} \quad y = 0, \quad \text{(B6)}$$

$$F \to 0 \quad \text{as} \quad y \to -\infty. \quad \text{(B7)}$$

In practice, because of the finiteness of the computer, the condition corresponding to (B7) must be applied at a finite distance L from the coast. An appropriate condition in terms of F is (see Brink, 1982b)

$$\frac{\partial}{\partial y}\left[\frac{fkF - F_y\omega}{f^2 - \omega^2}\right] = 0, \quad \text{at} \quad y = -L, \quad \text{(B8)}$$

where the term inside the brackets represents the velocity perpendicular to the coast.

In summary, the modal equations solved were (B2) subject to (B4)–(B6) and (B8).

REFERENCES

Battisti, D. S., and A. J. Clarke, 1982a: A simple method for estimating barotropic tidal currents on continental margins with specific application to the M_2 tide off the Atlantic and Pacific coasts of the United States. *J. Phys. Oceanogr.*, **12,** 8–16.

——, and ——, 1982b: Estimation of nearshore tidal currents on nonsmooth continental shelves. *J. Geophys. Res.*, **87,** 7873–7878.

Brink, K. H., 1982a: The effect of bottom friction on low-frequency coastal trapped waves. *J. Phys. Oceanogr.*, **12,** 127–133.

——, 1982b: A comparison of long coastal trapped wave theory with observations off Peru. *J. Phys. Oceanogr.*, **12,** 897–913.

Chapman, D. C., 1983: On the influence of stratification and continental shelf and slope topography on the dispersion of subinertial coastally trapped waves. *J. Phys. Oceanogr.*, **13,** 1641–1652.

——, and M. C. Hendershott, 1982: Shelf wave dispersion in a geophysical ocean. *Dyn. Atmos. Oceans,* **7,** 17–31.

Clarke, A. J., 1977: Observational and numerical evidence for wind-forced coastal trapped long waves. *J. Phys. Oceanogr.*, **7,** 231–247.

——, and D. S. Battisti, 1981: The effect of continental shelves on tides. *Deep-Sea Res.*, **28,** 665–682.

Duing, W., F. Ostapoff and J. Merle, 1980: *Physical Oceanography of the Tropical Atlantic during GATE.* UNESCO, Paris, France, 117 pp.

Fuglister, F. C., 1960: *Atlantic Ocean Atlas of Temperature and Salinity Profiles and Data from the International Geophysical Year of 1957–1958,* Vol. 1. Woods Hole Oceanographic Institution, Woods Hole, MA, 209 pp.

Gill, A. E., and A. J. Clarke, 1974: Wind-induced upwelling, coastal currents and sea-level changes. *Deep-Sea Res.*, **21,** 325–345.

Houghton, R. W., 1976: Circulation and hydrographic structure over the Ghana continental shelf during the 1974 upwelling. *J. Phys. Oceanogr.*, **6,** 909–924.

——, 1979: Characteristics of the fortnightly shelf wave along the Ghana coast. *J. Geophys. Res.*, **84,** 6355–6361.

——, and T. Beer, 1976: Wave propagation during the Ghana upwelling. *J. Geophys. Res.*, **81,** 4423–4429.

Huthnance, J. M., 1978: On coastal trapped waves: Analysis and numerical calculations by inverse iteration. *J. Phys. Oceanogr.*, **8,** 74–92.

Longhurst, A. R., 1962: A review of the oceanography of the Gulf of Guinea. *Bull. Inst. Francais d'Afrique Noire,* **A24,** 633–663.

Mysak, L. A., 1978a: Long period equatorial topographic waves. *J. Phys. Oceanogr.*, **8,** 302–314.

——, 1978b: Equatorial shelf waves on an exponential shelf profile. *J. Phys. Oceanogr.*, **8,** 458–467.

Ou, H. W., 1980: On the propagation of free topographic Rossby waves near continental margins. Part 1: Analytical model for a wedge. *J. Phys. Oceanogr.*, **10,** 1051–1060.

——, and R. C. Beardsley, 1980: On the propagation of free topographic Rossby waves near continental margins. Part 2: Numerical models. *J. Phys. Oceanogr.*, **10,** 1323–1339.

Philander, S. G. H., 1977: The effects of coastal geometry on equatorial waves (forced waves in the Gulf of Guinea). *J. Mar. Res.*, **35,** 509–523.

Picaut, J., 1983: Propagation of the seasonal upwelling in the eastern equatorial Atlantic. *J. Phys. Oceanogr.*, **13,** 18–37.

——, and J. M. Verstraete, 1979: Propagation of a 14.7-day wave along the northern coast of Guinea Gulf. *J. Phys. Oceanogr.*, **9,** 136–149.

Romea, R. D., and J. S. Allen, 1983: On vertically propagating coastal Kelvin waves at low latitudes. *J. Phys. Oceanogr.*, **13,** 1241–1254.

Wang, D.-P., and C. N. K. Mooers, 1976: Coastal-trapped waves in a continuously stratified ocean. *J. Phys. Oceanogr.*, **6,** 853–863.